On the classical dynamics of billiards on the sphere

1999 J. Phys. A: Math. Gen. 32 7803

(http://iopscience.iop.org/0305-4470/32/44/315)

J. Phys. A: Math. Gen. **32** (1999) 7803–7813. Printed in the UK PII: S0305-4470(99)03067-X

On the classical dynamics of billiards on the sphere

M E Spina and M Saraceno

Department of Physics, Comisión Nacional de Energía Atómica, Av. Libertador 8250, (1429) Buenos Aires, Argentina

Received 30 March 1999, in final form 21 July 1999

Abstract. We study the classical motion in bidimensional polygonal billiards on the sphere. In particular, we investigate the dynamics in tiling and generic rational and irrational equilateral triangles. Unlike the plane or the negative curvature cases we obtain a complex but regular dynamics.

1. Introduction

In this work we consider the classical motion of a point particle inside a two-dimensional polygonal billiard on a surface with constant positive curvature. Flat billiards and billiards on a surface with negative curvature have been extensively studied. It is well known that the dynamics in flat polygonal billiards depends on whether the inner angles of the polygon are rational multiples of π [1–3]. If this is the case these systems are referred to as 'pseudo-integrable' since they possess two constants of motion and the flow is restricted to a two-dimensional invariant surface. If at least one of the vertex angles is an irrational multiple of π the polygon is generically ergodic [4]. On the other hand, the interest in studying polygonal billiards on a surface with negative curvature is that the classical motion is simple and as chaotic as possible since the flow on these surfaces is hyperbolic [5].

By investigating the dynamics on a spherical surface we explore the other limit: instead of having more chaoticity, more focusing is expected with respect to the planar case as a consequence of the positive curvature. The motivation for studying these systems is to see how this focusing mechanism together with the compactness of the surface affects the classical motion. In particular, we will investigate the condition for integrability and stress the importance of tiling billiards. In the general case we will explore numerically the phase space portrait of curved polygonal billiards (i.e. periodic orbits, invariant surfaces, etc), and try to explain these numerical observations in a rather intuitive way. Another important observation is that the direct and the dual billiard problems become projective-dual on the sphere [6] and, hence, the problem we are considering is isomorphic to the polygonal dual billiard problem.

The paper is organized as follows. In section 2 we present the formalism and introduce the dual billiard problem. In section 3 we briefly discuss the case of billiards enclosed by meridians and parallels and then concentrate on the study of polygonal billiards, i.e. billiards whose boundary consists entirely of arcs of geodesics. In particular, we will focus on equilateral triangles. We will first study tiling triangles in section 3.1 and then generic triangles in section 3.2. For this we use the entry–exit map and finally make a comparison of small curved triangles with triangles on the plane. Conclusions are presented in section 4.

0305-4470/99/447803+11$30.00

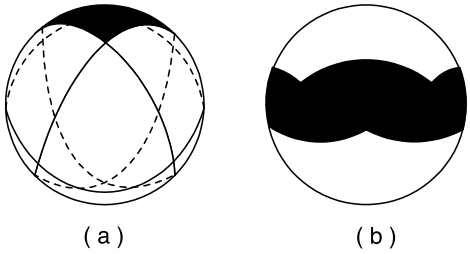

Figure 1. (*a*) Three intersecting geodesics enclosing a triangular billiard centred at the north pole. In (*b*) the shadowed area is the corresponding phase space on the dual space to the geodesics.

2. The model

The motion on the sphere will be described in terms of the spherical coordinates: the polar angle α and the azimuthal angle β. The coordinate curves $\alpha = \text{const}$ and $\beta = \text{const}$ form an orthogonal net. The line element for a sphere of radius R has the usual form:

$$\mathrm{d}s^2 = R^2\,\mathrm{d}\alpha^2 + R^2 \sin^2\alpha\,\mathrm{d}\beta^2 \tag{1}$$

and the curvature is $1/R^2$.

The geodesics are the great circles of the sphere and can be viewed as its intersection with a plane passing through the origin. They can be labelled by the coordinates (θ^G, ϕ^G) of the unit vector normal to this plane and their equation reads:

$$\tan\alpha = -\frac{\cot\theta^G}{\cos(\beta - \phi^G)}. \tag{2}$$

Note that α and β are coordinates on the physical sphere where the billiard lies while θ^G and ϕ^G denote a point on what is called the dual sphere. This is illustrated in figure 1. Since on the sphere the angle between lines is equal to the distance between the corresponding dual points the direct problem we are considering is isomorphic to the dual billiard map [6]. In other words, the dynamics of a particle moving along an oriented geodesic labelled by (θ^G, ϕ^G) and suffering specular reflections at the boundaries can be alternatively expressed as a map T acting on the point (θ^G, ϕ^G) on the dual sphere. This map reflects (θ^G, ϕ^G) in the point of tangency to the dual billiard, defined as the set of points dual to tangent lines to the direct billiard. It can be easily seen that the area element $\mathrm{d}A = \sin\theta\,\mathrm{d}\theta\,\mathrm{d}\phi$ is preserved by this bounce map T. Thus $\cos\theta^G$ and ϕ^G are canonical coordinates on the dual sphere. They provide a convenient reduced description of the classical motion alternative to the Birkhoff coordinates. In the plane the equivalent construction has been extensively studied, but it leads to two different dynamical systems, one for the direct billiard and one for its dual ([6] and references therein).

3. Polygonal billiards

The simplest systems on the sphere one can think of are convex billiards whose boundary consists of meridians ($\beta = \text{const}$) and parallels ($\alpha = \text{const}$). These are not polygons since parallels (except for the equator) are not geodesics. It is easy to see that in reflections on meridians and parallels, the quantity $\sin\theta^G$ is conserved. Therefore, the dynamics for these billiards is integrable. Depending on the initial conditions we get periodic and non-periodic orbits, giving rise to rational and irrational tori in phase space.

We now concentrate on polygonal billiards, i.e. systems enclosed by arcs of geodesics. Each of these arcs is a point on the dual sphere and, therefore, the dual billiard is also a polygon and the two dynamics are isomorphic.

For simplicity we will restrict our discussion to the case of equilateral triangles. While flat equilateral triangles are integrable, spherical equilateral triangles present a rich variety of possibilities depending on their size. This is due to the existence on the sphere of a definite relation between the size and the shape of the triangle. The inner angle ω can take any value in the interval $[\frac{\pi}{3}, \pi]$, and the area (that can be related to the total curvature) is: $A = R^2(3\omega - \pi)$.

For a triangle centred on the north pole the three sides will be specified by the vectors (θ^B, ϕ_i^B) which label the intersecting geodesics. Here, $\phi_i^B = (i-1)\frac{2\pi}{3}$ with $i = 1, 2, 3$, and the angle θ^B is related to the inner angle ω through

$$\sin\theta^B = \frac{\cos\frac{\omega}{2}}{\cos\frac{\pi}{6}}. \tag{3}$$

Points (θ^B, ϕ_i^B) define the dual triangle. Vertex V_i, defined as the intersection of geodesics $(i-1)$ and i, will be located at (α^V, β_i^V), where (α^V, β_i^V) denote coordinates on the physical sphere given by

$$\tan\alpha^V = \frac{2}{\tan\theta^B} \tag{4}$$

and

$$\beta_i^V = \phi_i^B + \frac{2\pi}{3}. \tag{5}$$

It will be useful in the following to introduce for each vertex V_i the curve C_i, the locus of the points (θ, ϕ) specifying all the geodesics passing by V_i. Its equation reads

$$\tan\theta_i = -\frac{\cot\alpha^V}{\cos(\phi_i - \beta_i^V)}. \tag{6}$$

It follows from equation (6) that curve C_i is itself a geodesic on the dual sphere labelled by (α^V, β_i^V). Note that this is not true in general but rather a consequence of the metric of our problem that will play an important role when understanding the structure of phase space. Once we have defined the discontinuity curves C_i it is easy to see that a point (θ, ϕ) corresponds to a geodesic entering (exiting) side i if: $\theta_i(\phi) \leqslant \theta \leqslant \theta_{i+1}(\phi)$ $(\theta_{i+1}(\phi) \leqslant \theta \leqslant \theta_i(\phi))$.

The area-preserving mapping T can be written explicitly as an orthogonal matrix acting on the unit vector $\begin{pmatrix}\sin\theta\cos\phi\\ \sin\theta\sin\phi\\ \cos\theta\end{pmatrix}$ as

$$T = T_i = \begin{pmatrix}\cos\phi_i^B & -\sin\phi_i^B & 0\\ \sin\phi_i^B & \cos\phi_i^B & 0\\ 0 & 0 & 1\end{pmatrix}\cdot\begin{pmatrix}-\cos 2\theta^B & 0 & \sin 2\theta^B\\ 0 & -1 & 0\\ \sin 2\theta^B & 0 & \cos 2\theta^B\end{pmatrix}\cdot\begin{pmatrix}\cos\phi_i^B & \sin\phi_i^B & 0\\ -\sin\phi_i^B & \cos\phi_i^B & 0\\ 0 & 0 & 1\end{pmatrix} \tag{7}$$

for $\theta_i(\phi) \leqslant \theta \leqslant \theta_{i+1}(\phi)$, that is for a geodesic entering side i or, alternatively, for a point (θ, ϕ) reflecting in (θ^B, ϕ_i^B).

Since the problem is symmetric under rotations in $\frac{2\pi}{3}$ around the centre of the triangles it will be useful to define the operators T^+ and T^- as

$$T^{\pm} = \begin{pmatrix}\cos\frac{2\pi}{3} & \pm\sin\frac{2\pi}{3} & 0\\ \mp\sin\frac{2\pi}{3} & \cos\frac{2\pi}{3} & 0\\ 0 & 0 & 1\end{pmatrix}\cdot\begin{pmatrix}-\cos 2\theta^B & 0 & \sin 2\theta^B\\ 0 & -1 & 0\\ \sin 2\theta^B & 0 & \cos 2\theta^B\end{pmatrix}. \tag{8}$$

With this definition, according to which, for example, $T_3T_2T_1 = T^+T^+T^+$ and $T_2T_1 = T^+T^-$, we indicate if the particle exiting from a given side hits the next or the previous side in increasing order with i.

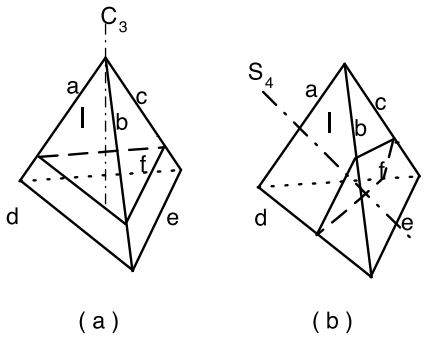

Figure 2. (*a*) Schematic diagram of a circuit visiting three faces of the tetrahedron, corresponding to an orbit of type $[\cdots+-\cdots]$ in triangle I. In (*b*) a circuit visiting four faces, associated to an orbit of type $[\cdots+++\cdots]$ is shown.

The trajectories in the triangle will be classified according to an infinite symbol sequence obtained by listing the sides successively hit. The code alphabet will consist of $+$, $-$ signs. This classification, as we will see, is not one to one in the sense that even infinite length sequences do not distinguish single trajectories uniquely.

3.1. Tiling triangles

We now study the case of equilateral triangles that tile the sphere under the reflection rule. Since the rotation group has a finite number of discrete subgroups there are only a few ways of tessellating the sphere. Tiling triangles are such that their vertices coincide with those of a face of a regular polyhedron. The three possible cases are the tetrahedron with $\omega = \frac{2\pi}{3}$, the octahedron with $\omega = \frac{\pi}{2}$ and the icosahedron with $\omega = \frac{2\pi}{5}$. We will see that tiling triangles constitute a very particular class of billiards that not only are integrable but for which only periodic orbits are present.

To study the motion in these three particular triangles we follow the procedure presented in [1]: every time an edge is hit, instead of reflecting the incident geodesic, we reflect the billiard across the edge and follow the same geodesic into the replica. That is, the motion is viewed as a unique geodesic entering and exiting copies of the original billiard. Since the surface is compact and the billiard is tiling it is clear that only periodic orbits exist. In order to determine their periodicity, n_p, we have to fold back, for each copy, the corresponding segment of geodesic into the original billiard. When, after a certain number of these operations, the image coincides with the original the trajectory closes. To do this we have to consider the symmetry group of the corresponding polyhedron and the possible circuits on it, that is, which faces are visited by the geodesic.

Triangle with $\omega = \frac{2\pi}{3}$. Two circuits are possible on the projected tetrahedron: one visits three faces, corresponding to orbits of type $[\cdots+-\cdots]$ in the triangular billiard, and the other visits four, corresponding to orbits $[\cdots+++\cdots]$. Both circuits are indicated in figure 2, where the notation for the tetrahedron is defined. Sides are indicated with $a, b, c \ldots$, while with $\sigma_a, \sigma_b, \sigma_c \ldots$ we denote reflections across these sides. Face I corresponds to the original billiard.

The orbits of the first type correspond to following a geodesic passing through faces $I, \sigma_b I, \sigma_c\sigma_b I, \sigma_a\sigma_c\sigma_b I, \ldots$. The transformation $\sigma_j\sigma_i$ is a rotation C_3^2 through $\frac{4\pi}{3}$ about the line of intersection of the reflection planes. Thus the product of six reflections, corresponding to a rotation in 4π, brings back the segment of the geodesic to its original position and orientation. Therefore, general periodic orbits of type $[\cdots+-\cdots]$ have periodicity $n_p = 6$.

There are three particular orbits of lower periodicity $n_p = 2$. These are the ones invariant under the rotation around three of the four C_3 axes of the tethahedron, that is, the geodesics resulting from the intersection with the sphere of the planes orthogonal to these axes.

The orbits of type $[\cdots+++\cdots]$ correspond to a geodesic passing through faces $I, \sigma_b I, \sigma_c\sigma_b I, \sigma_f\sigma_c\sigma_b I, \sigma_a\sigma_f\sigma_c\sigma_b I, \ldots$. It can be seen that the product of three reflections $\sigma_k\sigma_j\sigma_i$ is a rotary-reflection S_4 about one of the binary axes joining the centres of two opposite sides of the tetrahedron, as shown in figure 2. Since $(S_4)^4 = E$, 12 reflections are needed in order to recover the initial segment of geodesic in the original billiard and the periodicity of the orbits will be $n_p = 12$. There is, finally, an orbit with periodicity $n_p = 3$ that joins the centres of the three sides of the triangle.

Triangle with $\omega = \frac{\pi}{2}$. Due to the geometry of the octahedron, all the trajectories in this triangle are of the type $[\cdots+++\cdots]$. A product of three reflections is equivalent to an inversion, transforming θ^G, ϕ in $\pi - \theta, \phi + \pi$. Since any geodesic is invariant under this operation, the periodicity for all the orbits will be $n_p = 3$.

Triangle with $\omega = \frac{2\pi}{5}$. Following the same procedure we find in this case orbits of type $[\cdots+++\cdots]$ which have, in general, periodicity $n_p = 15$ (and one with $n_p = 3$ that joins the centres of the three sides of the triangle) and orbits of the type $[\cdots++--\cdots]$ with $n_p = 12$ (and three orbits with lower periodicity $n_p = 4$).

One can also think of triangles that are not tiling in the strict sense but which, by successive reflections on their sides, cover the sphere more than once. This is the case of a triangle with $\omega = \frac{4\pi}{5}$ that covers the spherical surface twice. It has periodic orbits of type $[\cdots+-\cdots]$ with periodicity $n_p = 10$, of type $[\cdots+++\cdots]$ with periodicity $n_p = 15$ and of type $[\cdots++-++-++-\cdots]$ with periodicity $n_p = 9$.

3.2. Generic triangles

The entry–exit map. Let us now investigate the case of a generic triangle with an arbitrary θ^B. Following [7] we will divide the available phase space in the (θ, ϕ)- plane in entry (or exit) domains of the three sides. The entry (exit) domain is defined as the set of points associated with the oriented geodesics that enter (or exit) a given side. In order to do this partition, we use curves C_i, defined in equation (6).

In figure 3(*a*) we show an example of an entry–exit map. The intersections of curves C_i and C_{i-1} correspond to the points associated to side $i - 1$ with the two possible orientations. Each point in the available phase space belongs to one entry and one exit domain. Each exit domain is intersected by two entry domains.

After n iterations of the map according to equation (7) the phase space gets partitioned into domains which are enclosed by geodesics, since the images by reflection of the separating curves C_i are also geodesics. Each domain can be labelled by a sequence of n symbols denoting the n sides successively hit by the trajectories inside this domain.

The only general rule limiting the possible sequences is that a side cannot be hit twice consecutively. But it is clear that for each particular triangle the existence or absence of a region associated with a given sequence is determined by the geometry, in this case, the inner angle ω. For example the domain corresponding to an infinite periodic sequence of type $[\cdots+-\cdots]$ exists only in triangles with angle $\omega > \frac{\pi}{2}$.

Figure 3(*b*) shows the partition of phase space after two iterations of the map. As long as the number of iterations remains finite the different allowed domains are bounded by arcs of geodesics and therefore polygons of increasing complexity. When a given sequence of n_p

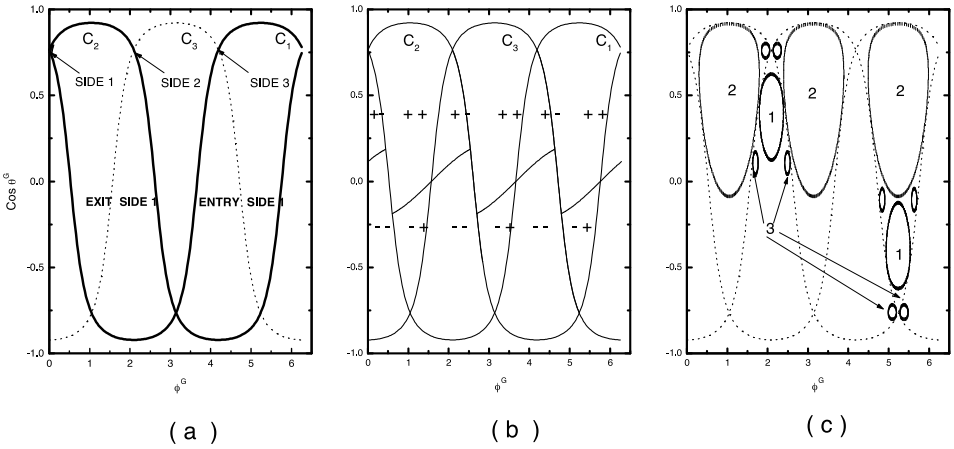

Figure 3. (*a*) Entry–exit map for a triangle with $\theta^B = 0.7$. (*b*) Phase space after two iterations become partitioned in domains corresponding to orbits of type [++] ([−−]) and of type [+−] ([−+]). (*c*) The domains corresponding to orbits $[\cdots +- \cdots]$ (1), $[\cdots +++ \cdots]$ (2) and $[\cdots ++++---- \cdots]$ (3) after infinite iterations.

symbols is repeated periodically an infinite number of times the resulting set of trajectories is a chain of n_p elliptic islands bounded by a smooth curve which is the limit of the above-mentioned polygons. Short repeated sequences lead to large and fairly regular areas, while long sequences lead to complex island chains. Since the period n_p can be arbitrarily large, the corresponding n_p islands can be arbitrarily small and, eventually, reduce to points (for infinite orbits). Figure 3(*c*) shows the domains corresponding to the repetition of some short codes.

Before studying the structure of these islands in more detail, let us have a look at the entry–exit maps for the special case of the tiling triangles treated in the previous section. The common feature to these particular triangles is that the corresponding separating geodesics C_i are reflected into themselves after a few iterations. Therefore, phase space gets partitioned into a few polygonal (in the sense that they are enclosed by a finite number of segments of geodesics) domains corresponding to different periodic codes. Inside each domain, all orbits are periodic with the same periodicity and we recover the result obtained in the previous section. This is illustrated in figure 4. Generic non-tiling triangles may have domains in which all trajectories are periodic, coexisting with the families of elliptic islands. These triangles with periodic domains can be found by requiring the angle θ^B to be such that successive applications of the bouncing matrix corresponding to a chosen sequence gives the unit matrix. For example, requiring that $(T^+T^+T^+)^n = I$ gives

$$\theta^B = \arccos \frac{\cos \frac{k\pi}{n}}{\cos \frac{\pi}{6}} \tag{9}$$

while $(T^+T^-)^n = I$ fixes

$$\theta^B = \arcsin \frac{\cos \frac{2k\pi}{3n}}{\cos \frac{\pi}{6}} \tag{10}$$

where k and n are integers.

Thus, if a triangle defined by θ^B and its complement, i.e., the one defined by $\frac{\pi}{2} - \theta^B$ have inner angles ω_1 and ω_2 which are both rational, angle θ^B satisfies simultaneously equations (9) and (10) and the pair of rational angles (ω_1, ω_2) fulfil

$$\cos \omega_1 + \cos \omega_2 = -\tfrac{1}{2}. \tag{11}$$

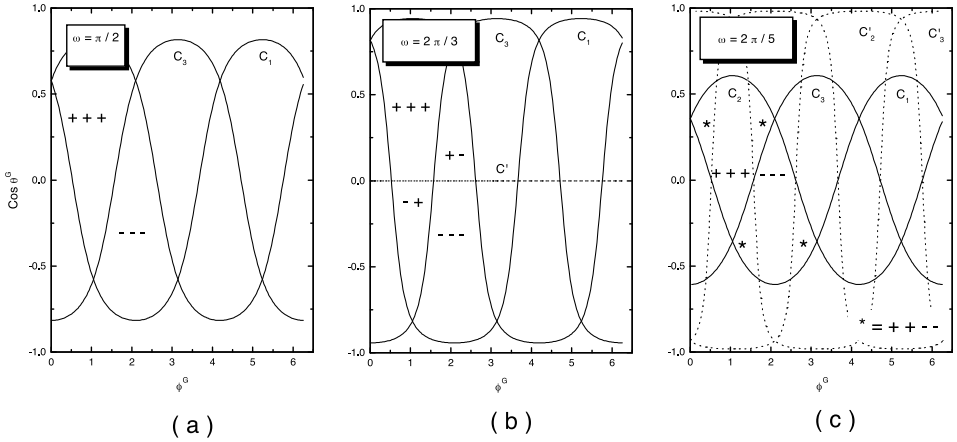

Figure 4. Phase space portrait for tiling triangles. (*a*) For $\omega = \frac{\pi}{2}$ curves C_i reflect into themselves. (*b*) For $\omega = \frac{2\pi}{3}$ curves C_i reflect into C' ($\theta^B = \frac{\pi}{2}$). (*c*) For $\omega = \frac{2\pi}{5}$ curves C_i reflect into C_i' which, in turn, reflect again into C_i.

We found numerically two pairs of rational angles satisfying equation (11): ($\omega_1 = \frac{\pi}{2}, \omega_2 = \frac{2\pi}{3}$) and ($\omega_1 = \frac{2\pi}{5}, \omega_2 = \frac{4\pi}{5}$), corresponding to the triangles analysed in the previous section.

Summarizing, we see that the entry–exit map is a useful tool to determine whether, according to the geometry (in this simple case the inner angle ω), a domain corresponding to a given code exists or not in a given triangle. For this it is sufficient to reflect the segments of the separating geodesics C_i enclosing the initial domain according to the chosen sequence. The image domain after infinite iterations can be either empty, finite or reduced to a single point, in contrast with the hyperbolic case where non-empty domains associated to a code are always reduced to a single point. Finite domains are in general bounded by smooth curves, resulting from the intersection of an infinite number of geodesics. In generic triangles some particular codes are associated to polygonal domains enclosed by a finite number of geodesics.

The structure of phase space. In order to understand the detailed structure of phase space in the generic case we now follow individual trajectories. A phase space plot is shown in figure 5 for different initial conditions. It reminds one very much of the stable regime of a sawtooth map [8]. At the centre of each island, belonging to a set of n_p islands, sits a periodic orbit of period n_p surrounded by a family of nested invariant curves. These correspond to open orbits having the same dynamics as the central periodic orbit, i.e., they follow the same periodic sequence or reflections. Therefore, a given code does not specify a single trajectory, as in the hyperbolic case, but an entire family of orbits. The size of the islands decreases as n_p increases and phase space takes a fractal structure.

The existence of these islands is a consequence of the focusing mechanism on the spherical surface. The fact that two geodesics on the sphere intersecting at θ_{int}, ϕ_{int} cross again at $\pi - \theta_{int}, \phi_{int} + \pi$ reflects on the structure of the orbits. To illustrate this we consider a periodic orbit with initial conditions ($s^{p.o.}, p_{\parallel}^{p.o.}$) expressed in Birkhoff coordinates and an open trajectory close to it. If the initial conditions are close enough to the ones of the periodic orbit the particle on the open trajectory will follow the sequence of the periodic orbit and, after a period, end at a point s on the boundary that is shifted with respect to the point $s^{p.o.}$. The position s as a function of the number of period iterations is plotted in figure 6 for a given orbit in a curved and a flat triangle of equal area. In the flat billiard the shift $s - s^{p.o.}$ increases

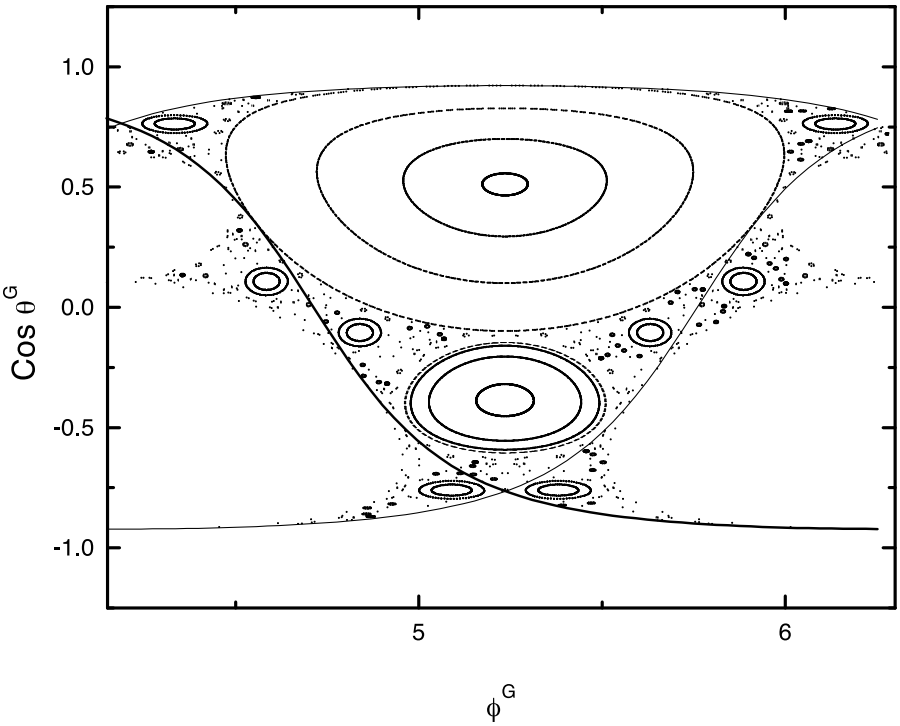

Figure 5. Phase space plot for a triangle with $\theta^B = 0.7$. 20 orbits are shown, each iterated 1000 times.

linearly, in such a way that, after a certain number of iterations, the vertex will eventually be reached and the original sequence broken. In the spherical case the shift is an oscillatory function of the number of iterations. If the amplitude of oscillation is small enough the corner is never reached: the pendulating motion lasts forever and the particle keeps repeating the original symbolic sequence but never retracing itself exactly. As long as the concentric curves do not become tangent to curves C_i, that act as separatrices, the open trajectories have the same code as the central periodic orbit. The corresponding transformation is a product of a string of orthogonal matrices T_i. The resulting 3×3 matrix is itself orthogonal and therefore has an eigenvalue 1, corresponding to preservation of the norm, and a pair of complex conjugate phases $e^{\pm i\Omega}$. Thus, the motion inside an island is labelled by a code and is everywhere elliptic with the same rotation angle Ω. This is clearly displayed in figure 5. The only mechanism to distinguish the evolution of initially close trajectories is the intersection with curves C_i. In fact, when the outer curve becomes tangent to C_i, the original sequence is broken and a new and more complex sequence appears, corresponding to a new chain of islands.

This is an example of a piecewise linear discontinous map. Its general features present some similarities with the polygonal dual map in the plane. In both cases the structure of phase space is determined by the set of curves that will eventually feel the discontinuity of the map: in our case curves C_i and their successive reflections. These draw a complicated pattern, enclosing finite domains that might reduce to single points in the case of infinite orbits. The main difference between both cases is that in the plane these domains are polygonal and all orbits in them are periodic, while in the sphere they consist of a single central periodic orbit and a set of concentric open orbits sharing the same dynamics. Within these open domains that

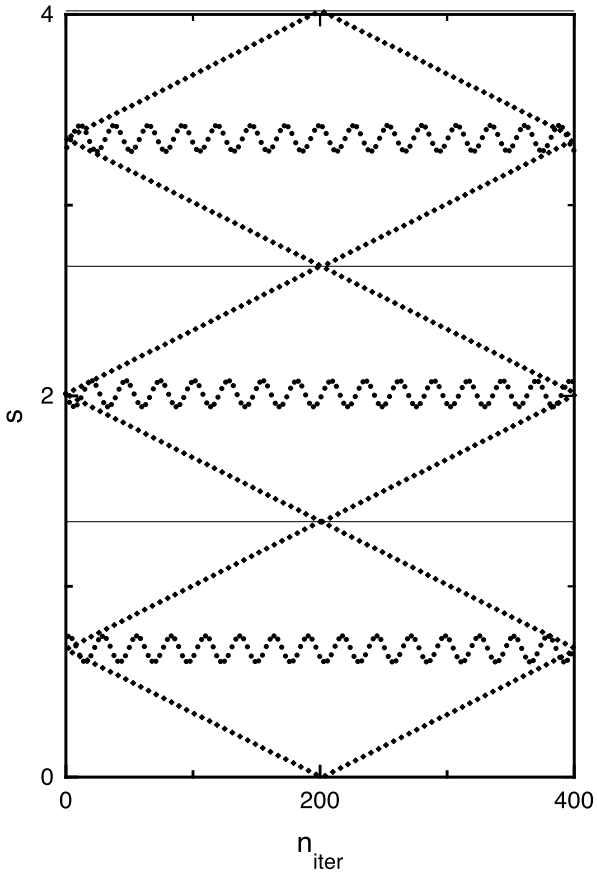

Figure 6. Position on the boundary s plotted as a function of the number of iterations for an open trajectory in the neighbourhood of a periodic orbit of period $n_p = 3$, starting at $s^{p.o.}$. Dots correspond to the curved triangle, diamonds to the planar triangle of equal area. Horizontal lines indicate the edges.

correspond to a finite allowed symbolic sequence the motion is integrable, with rotation angle given by the eigenvalue of the correponding orthogonal matrix. Some properties of the set of infinite orbits have been investigated for planar polygons [6, 9] and need further investigation in the spherical case.

Small triangles. If we go to the limit of small triangles the total curvature can be seen as a perturbation from the integrable case of flat equilateral triangles. This limit corresponds to taking $\omega \to \frac{\pi}{3}$, (that is $\theta^B = \frac{\pi}{2} - \epsilon$). This restricts the available space phase to geodesics with θ^G close to $\frac{\pi}{2}$. For the segments inside the billiard, that is β in a small interval around $\phi^G + \pi$, the equation of the geodesics reads

$$\alpha = \frac{\theta^0}{\cos(\beta - \phi^0)} \tag{12}$$

where $\theta^0 = \frac{\pi}{2} - \theta^G = \epsilon$ and $\phi^0 = \phi^G + \pi$, that is, the equation of a straight line in polar coordinates in the plane.

The reflection across a side of the planar triangle is given by

$$\alpha' = -\alpha + 2\theta_0 \cos(\beta - \phi^0) \tag{13}$$

$$\beta' = -\beta + 2\phi_0 \tag{14}$$

which can also be obtained by expanding equation (7) to first order in ϵ. All trajectories lie on tori-filling phase space. In figure 7(*a*) several rational and irrational tori are shown. Under

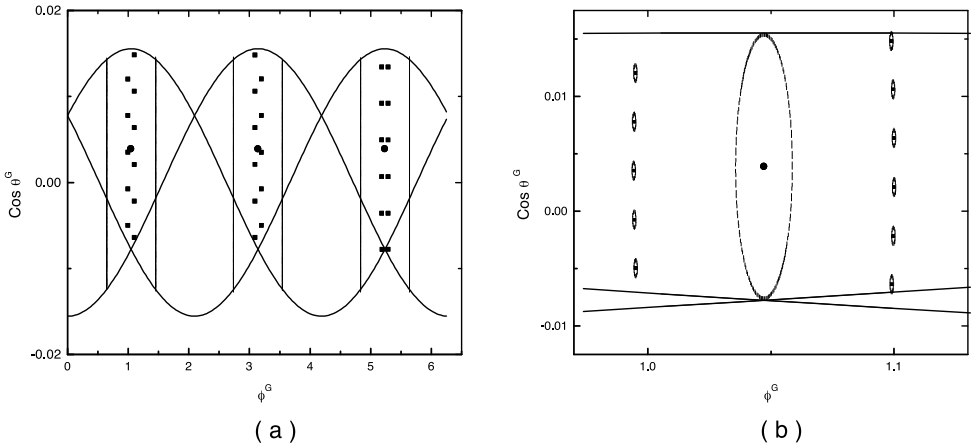

Figure 7. (*a*) Some tori in a planar triangle. Circles correspond to a rational torus with $n_p = 3$, squares to $n_p = 34$ and the straight line to an irrational torus. (*b*) For a curved triangle with $\omega = \frac{10\,001\pi}{30\,000}$ open trajectories develop around the elliptic points.

perturbation, these rational tori are destroyed and the fixed points that survive perturbation are all stable as a consequence of the focusing mechanism due to the positive curvature. Around each stable point of the periodic orbit, n_p, a family of invariant curves, corresponding to open trajectories, develops. This is shown in figure 7(*b*).

Note that due to the isomorphism of the direct and dual system on the sphere we could also consider as an unperturbed system the planar triangular dual billiard, which is also integrable and exhibits only periodic orbits.

4. Conclusions

This work was a first step in the understanding of the classical dynamics in billiards on a spherical surface. We only considered polygonal billiards and, more specifically, equilateral rational and irrational triangles. The main conclusion is that all periodic orbits are stable and they are surrounded by open regions of elliptic type characterized by an infinite repeating code. This is a consequence of the focusing mechanism and constitutes a substantial difference with respect to the planar and hyperbolic cases where each infinite code is associated to a single orbit. The map has a regular but very complex structure. The phase space is covered by chains of elliptic islands, whose multiplicity increases and size decreases with the period, infinite orbits corresponding to unstable points. The structure of the set of orbits with infinite non-repeating codes remains to be explored. Tiling billiards constitute a very special system where only periodic orbits are present. We have also studied non-equilateral triangles and the general structure of phase space is very similar. We do expect differences if the boundaries are not geodesics: in particular, the motion is likely to develop large chaotic regions. Conditions for hyperbolicity of billiards on surfaces of constant curvature have been recently studied in [10]. This question together with the issues of quantization will be addressed in the future.

Acknowledgments

We are grateful to the referees who pointed out valuable references. This work was partially supported by PICT97 03-00050-01015 and CONICET PIP 0420/98.

References

[1] Richens P J and Berry M V 1981 *Physica* D **2** 495
[2] Gutkin E 1986 *Physica* D **19** 311
[3] Gutkin E 1996 *J. Stat. Phys.* **83** 7
[4] Kerckhoff S, Masur H and Smillie J 1986 *Ann. Math.* **124** 293
[5] Balazs N L and Voros A 1986 *Phys. Rep.* **143** 109
[6] Tabachnikov S 1995 *Adv. Math.* **115** 221
[7] Giannoni M-J and Ullmo D 1990 *Physica* D **41** 371
[8] Lakshminarayan A and Balazs N L 1995 *Chaos Solitons Fractals* **5** 1169
[9] Vivaldi F and Shaidenko A V 1987 *Commun. Math. Phys.* **110** 625
[10] Gutkin B, Smilansky U and Gutkin E 1999 *Preprint* chao-dyn/9905030